

## Supporting Information

**Title:** Hydrogel micropost arrays with single post tunability to study cell volume and mechanotransduction

**Authors:** Daniel Devine<sup>1,2#</sup>, Vishwaarth Vijayakumar<sup>1,2#</sup>, Sing Wan Wong<sup>1,2#</sup>, Stephen Lenzini<sup>1,2</sup>, Peter Newman<sup>1,2+</sup>, Jae-Won Shin<sup>1,2\*</sup>

### Affiliations:

<sup>1</sup>Department of Pharmacology and Regenerative Medicine, University of Illinois at Chicago, Chicago, IL, USA

<sup>2</sup>Department of Bioengineering, University of Illinois at Chicago, Chicago, IL, USA

<sup>#</sup>Equal contribution

<sup>+</sup>Current address: University of Sydney, Sydney, Australia

<sup>\*</sup>Correspondence to J-W. S.: [shinjaw@uic.edu](mailto:shinjaw@uic.edu)

**Keywords:** mechanobiology; extracellular matrix; cell volume; hydrogels; microposts

This file contains:

Supporting Figures 1-6

## Supporting Figures

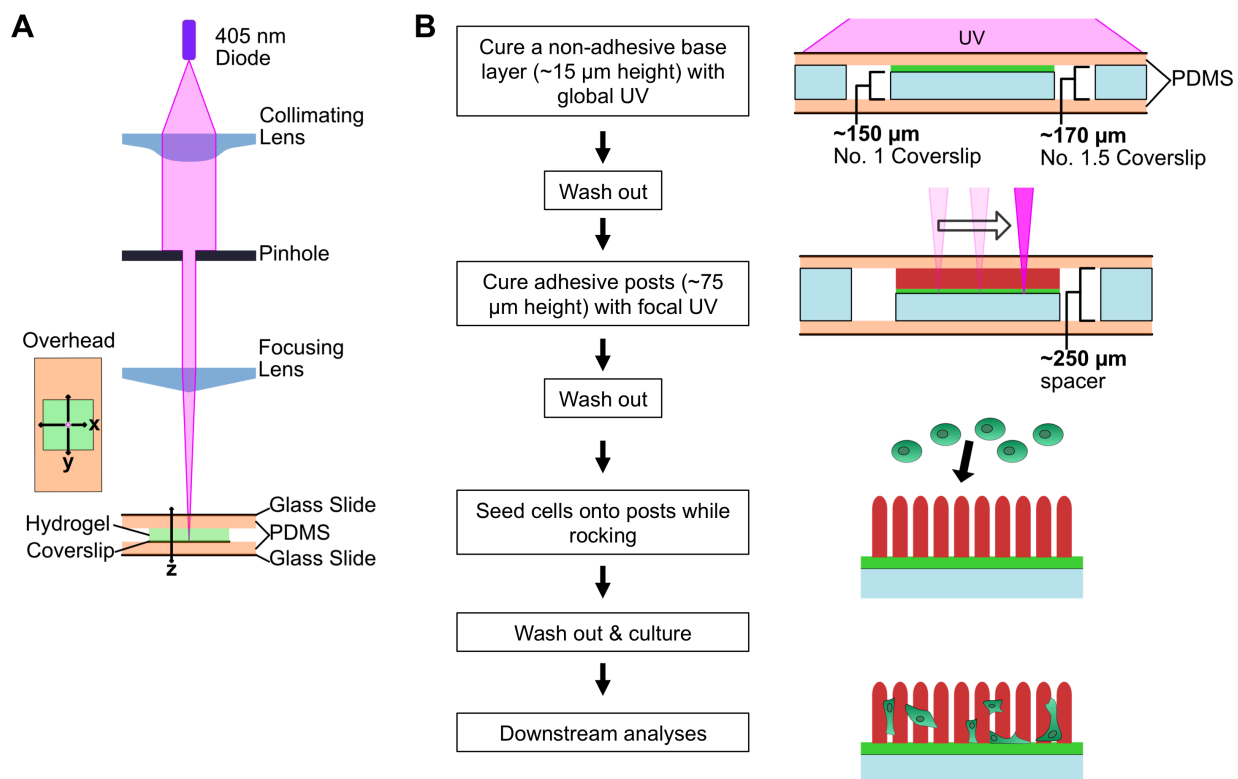


**Figure S1. Freeform stereolithography.** (A) Schematic illustration of custom print head and scaffold printing chamber used to print microposts. (B) General process flow used to print micropost scaffolds and use for biological experiments, with schematic illustration of print chamber during base layer and post fabrication. The base layer was cured by UV lamp exposure for 90 seconds, and washed three times with post hydrogel solution prior to printing microposts with cRGD-containing hydrogel. All hydrogels were washed out for 1-3 days prior to experiments.

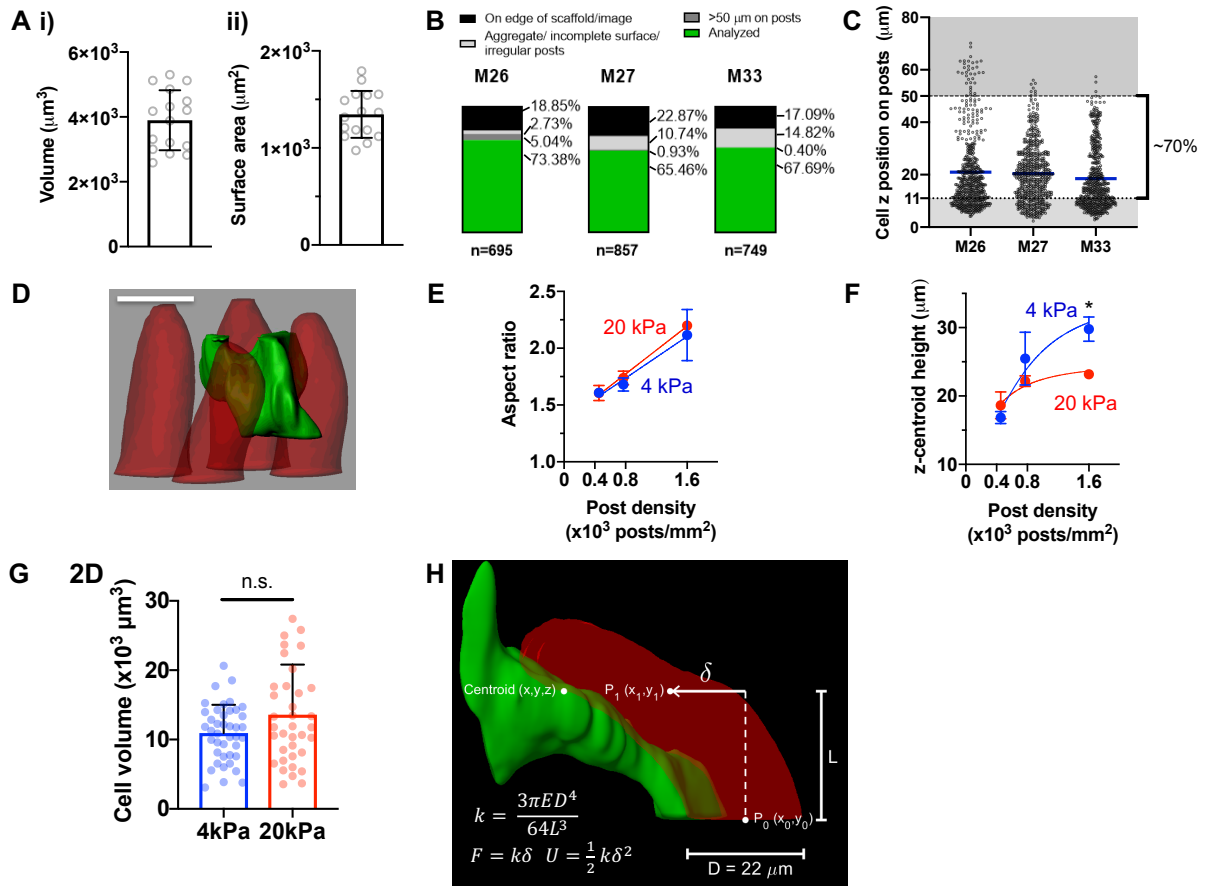


**Figure S2. Characterization of MSCs in hydrogel micropost arrays.** (A) (i) Volume and (ii) surface area of individual MSCs immediately after (<2 h) embedded in collagen;  $n = 16$ . Error bars: SD. (B) Exclusion analysis of cells from 3 donors. 3D reconstruction of cells from confocal images was done in Imaris based on fluorescence intensity of CellMask Green plasma membrane stain. Cells attached to scaffold boundary or clipped at edge of the confocal image were excluded from analysis. Cells were further excluded due to aggregation (2 or more cells in contact), incomplete membrane stain/surface rendering, primarily contacting irregular posts, or being located outside the linear cell attachment region (> 50  $\mu\text{m}$  in height from the post base). (C) Distribution of cell positions along the posts after 24h culture. Cell positions are defined as the centroid z coordinate (mean vertical position) relative to post base positions. 2.9% of all cells were located outside the linear cell attachment region of the post, while ~70% of all cells were located between 11-50  $\mu\text{m}$ ;  $n \geq 695$  per donor. (D) Representative images showing a live MSC located in the interstitial spaces between microposts above a base layer. Scale bar = 25  $\mu\text{m}$ . (E) Aspect ratio of MSCs. Points were fit to linear regression,  $Y = Y_0 + AX$ . ( $Y_0$ ,  $A$ ) values for 4 kPa = (1.37, 459.4), for 20 kPa = (1.35, 525.9). (F) Average centroid z height of MSCs. Dose response fit (Fig. 2) values (min, max, potency, b) for 4 kPa = (11, 35, 729, 1.96), for 20 kPa = (11, 25, 387, 1.56). For (E) and (F), data points were plotted as a function of post density in 4-kPa or 20-kPa arrays. \* $p < 0.05$ , two-way repeated measures ANOVA followed by Tukey's multiple comparisons test. Error bars represent the SEM of the mean values across 3 different MSC donors.  $n \geq 70$  cells per donor. (G) Cell volume on 2D PEG-DA gels with cRGD. Error bars: SD;  $n \geq 37$  cells pooled from 3 independent experiments. (H) Illustration of the approach used to calculate the Hookean force and strain energy that cells applied to bend posts.  $k$ , the spring constant, was defined in terms of  $E$ , the elastic modulus of the post (4 or 20 kPa);  $D$ , the diameter of the post; and  $L$ , the height of the centroid of the cell from the base of the post in the  $z$  direction.  $\delta$ , the deflection of the post, was measured between the centroid of the base of the post ( $P_0$ ) and the centroid of the post at the  $z$ -stack image corresponding to the height of the centroid of the cell ( $P_1$ ).

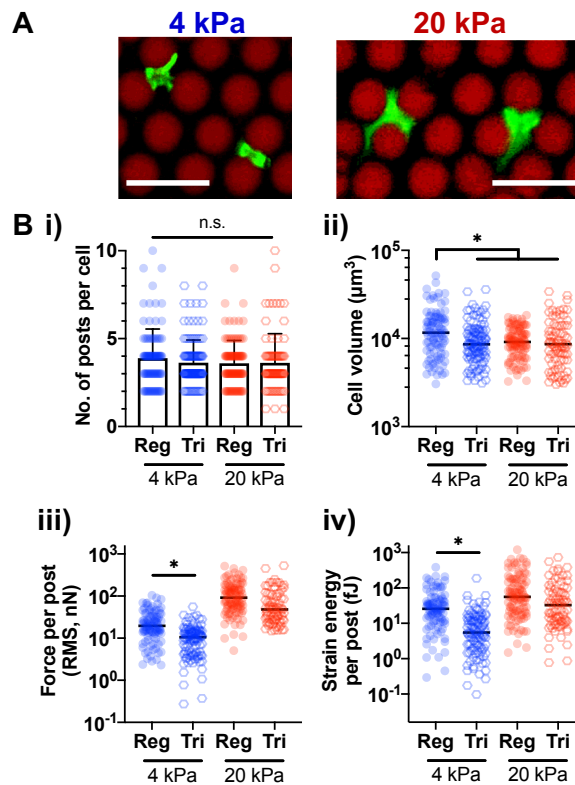


**Figure S3. Characterization of cell volume, traction force and strain energy in arrays with triangular post arrangement.** (A) Representative image showing live MSCs seeded in triangular micropost arrays. Scale bar = 50  $\mu\text{m}$ . (B) Quantification of (i) number of posts per cell, (ii) cell volume, (iii) average force per post, (iv) strain energy per post. Reg: regular array, Tri: triangular array.  $*p < 0.05$ , Kruskal-Wallis test, followed by Dunn's multiple comparisons test. Error bars in (i) represent SD, and median values are shown in (ii)-(iv);  $n \geq 85$  for each group pooled from 3 independent experiments, 1 donor.

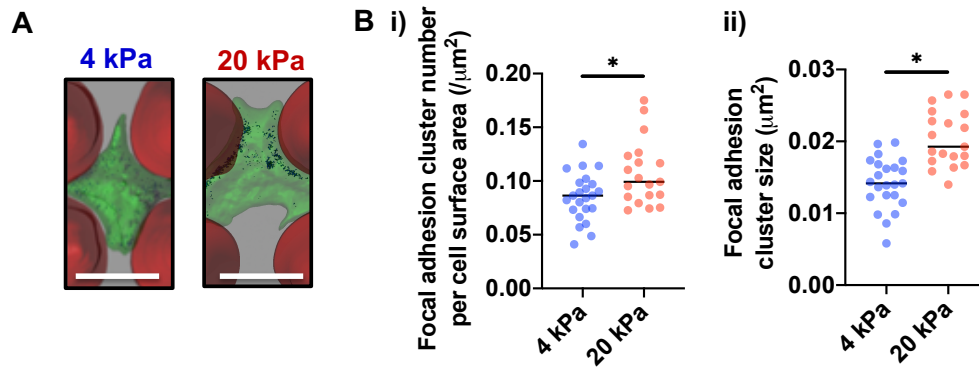


**Figure S4. Quantification of paxillin<sup>+</sup> focal adhesion in MSCs adhered to micropost arrays. (A)** Representative images showing live MSCs (transparent green, labelled with plasma membrane stain) that express paxillin-RFP puncta (dark green) in micropost arrays (red). Scale bar = 20  $\mu\text{m}$ . **(B)** Quantification of paxillin-RFP puncta in terms of (i) cluster number per cell surface area, and (ii) average cluster size per cell. \* $p < 0.05$ , two-tailed Welch's T-test. Median values are shown for each group;  $n \geq 20$  cells for each group pooled from 3 independent experiments, 1 donor.

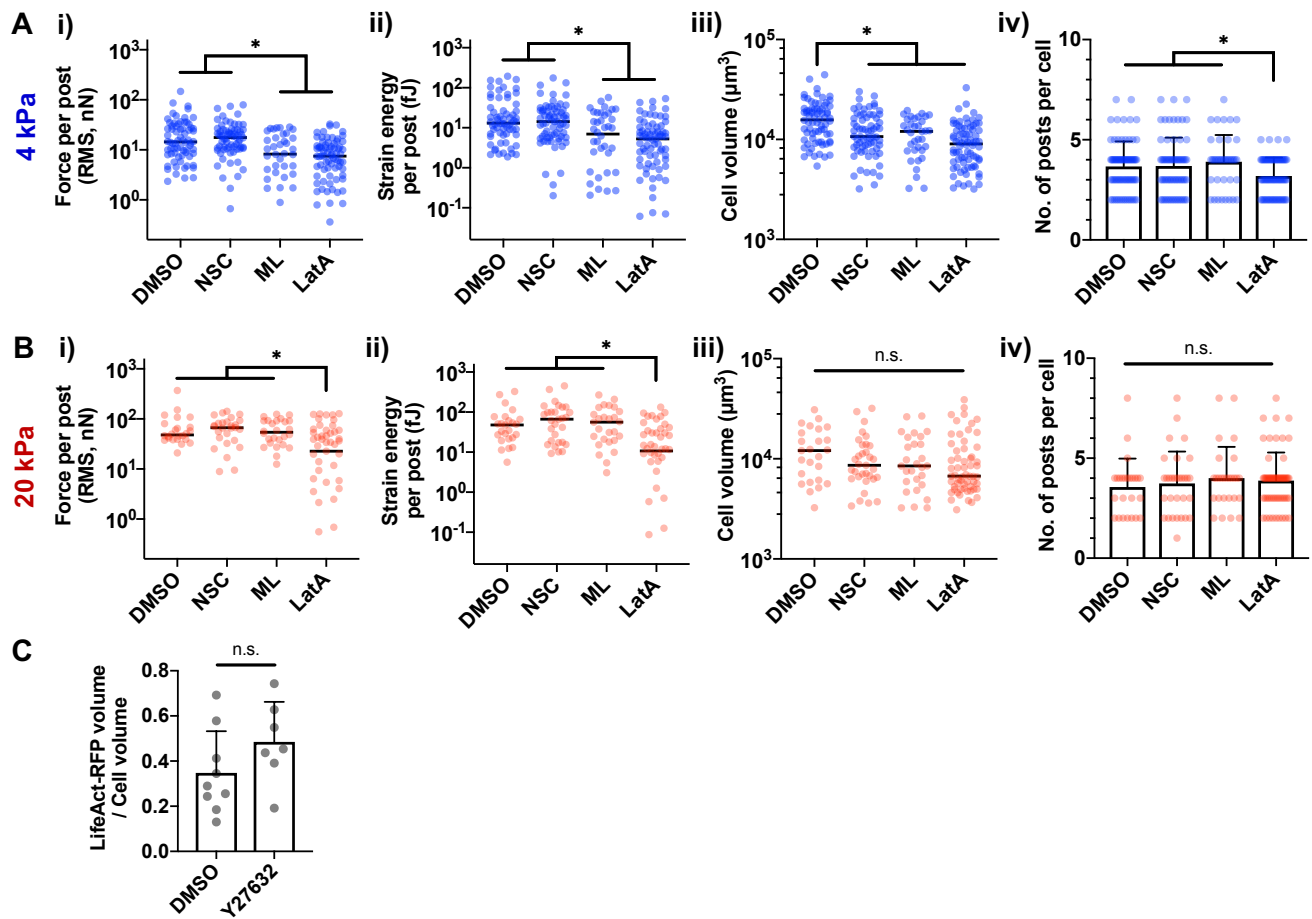


**Figure S5. Effects of Rac, Cdc42 and actin polymerization on MSCs in micropost arrays.** MSCs in micropost arrays were treated with DMSO, the Rac inhibitor NSC23766 (“NSC”, 10  $\mu\text{M}$ ), the Cdc42 inhibitor ML141 (“ML”, 10  $\mu\text{M}$ ) or latrunculin A (“Lata”, 0.25  $\mu\text{M}$ ) for 4 hours prior to analysis. Effects of inhibitors on MSCs in (A) 4-kPa arrays and (B) 20-kPa arrays. For (A) and (B), (i) average force per post, (ii) average strain energy per post, (iii) cell volume, (iv) number of interacting posts per cell. \* $p < 0.05$ , Kruskal-Wallis test, followed by Dunn’s multiple comparisons test. For (i)-(iii), median values are shown, and error bars in (iv) represent SD.  $n \geq 25$  for each group pooled from 2 independent experiments, 1 donor. (C) Quantification of F-actin in live MSCs. After transfection with LifeAct-RFP, MSCs were seeded in 4-kPa arrays for 24 hours, followed by treatment with DMSO or Y27632 for 24 hours;  $n \geq 7$  cells for each group.

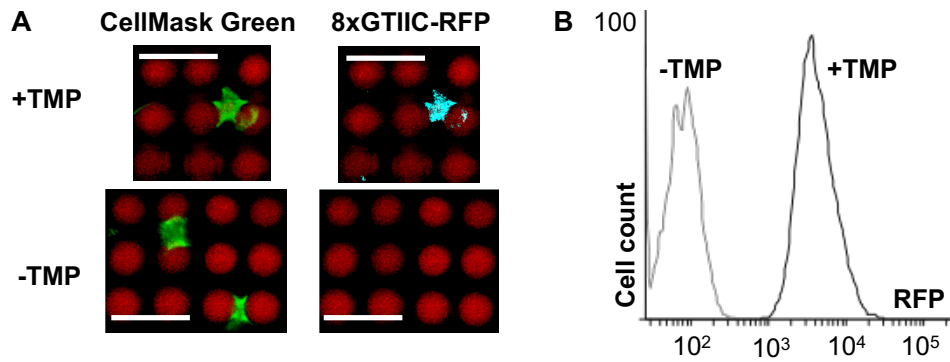


**Figure S6. YAP-responsive reporter expression. (A)** Representative images showing YAP reporter transfected MSCs in 20-kPa posts. CellMask Green: plasma membrane, 8xGTIIC-RFP: RFP reporter expressed as a function of YAP activity on the 8XGTIIC promoter. RFP is fused with a destabilization domain (DD) that is stabilized only in the presence of trimethoprim (TMP). Thus, RFP signals are not detectable above the background level in the absence of TMP. Scale bar = 50  $\mu\text{m}$ . **(B)** Representative flow cytometry histogram showing cell population of YAP reporter transfected MSCs with or without TMP.